International Journal of Applied Pharmaceutics

ISSN- 0975-7058 Vol 16, Issue 4, 2024

Original Article

IDENTIFICATION OF BENZYLIDENE AMINO PHENOL INHIBITORS TARGETING THYMIDYLATE KINASE FOR COLON CANCER TREATMENT THROUGH IN SILICO STUDIES

MOHD ABDUL BAQI[1], KOPPULA JAYANTHI[2], RAJESH KUMAR R.[1*]

[1,3]Department of Pharmaceutical Biotechnology, JSS College of Pharmacy, JSS Academy of Higher Education and Research, Ooty, Nilgiris, Tamil Nadu, India. [2]Department of Pharmaceutical Chemistry, JSS College of Pharmacy, JSS Academy of Higher Education and Research, Ooty, Nilgiris, Tamil Nadu, India

*Corresponding author: Rajesh Kumar R.; Email: bathmic@jssuni.edu.in

Received: 14 Nov 2023, Revised and Accepted: 24 Apr 2024

ABSTRACT

Objective: Thymidylate kinase (TMK) is pivotal in bacterial DNA synthesis, facilitating the conversion of Deoxythymidine Monophosphate (dTMP) into Deoxythymidine Diphosphate (dTDP). This crucial role positions TMK as an attractive target for the creation of innovative anti-cancer therapies. To date, there have been no anti-cancer medications developed specifically targeting this enzyme.

Methods: The investigation involved screening benzylidene derivatives as potential ligands for their efficacy. This process was executed through the utilization of the Glide module for molecular docking, followed by an Absorption, Distribution, Metabolism, and Excretion (ADME) analysis via Qikprop. Subsequently, the Prime Molecular Mechanics-Generalized Born Surface Area (MM-GBSA) approach was employed to evaluate the binding free energy of these ligands. To further assess the stability of these ligands as inhibitors of Human Thymidylate Kinase (HaTMK), molecular dynamics (MD) simulations were conducted over a 100 nanosecond timeframe.

Results: Among the screened molecules, ten exhibited significant binding affinity, engaging in hydrogen and hydrophobic interactions with the Asp15, Phe105, and Phe72 residues of the HaTMK enzyme (PDB ID: 1E2D). Notably, the molecule 4-((4-dichlorobenzylidene) amino) phenol demonstrated the highest docking score with an Extra Precision (XP)-docking value of −6.33 kcal/mol, indicating a strong binding affinity based on extra-precision docking. Further analysis through Prime MM-GBSA revealed notable binding energies, including a ΔG_{Bind} of −52.98 kcal/mol, ΔG_{Lipo} of −27.75 kcal/mol, and ΔG_{VdW} of −47.70kcal/mol, suggesting significant interaction strength. Throughout the MD simulations, interactions between the ligand and the Glu152 and Phe105 residues remained stable, underlining the molecule's potential as a TMK inhibitor.

Conclusion: The ligand 4-((4-dichlorobenzylidene) amino)phenol, characterized by its benzene ring, benzylidene moiety, and oxygen group, engages effectively with the HaTMK protein's active sites. This interaction showcases its promising potential as an inhibitor of HaTMK, positioning it as a viable candidate for the treatment of colon cancer.

Keywords: Thymidylate kinase (TMK), Molecular docking, Molecular dynamics (MD) simulations, MM-GBSA, High-throughput virtual screening (HTVS), ADME profiles, Cancer therapy, Colorectal cancer (CRC), Human thymidylate kinase (HaTMK)

DOI: https://dx.doi.org/10.22159/ijap.2024v16i4.50874 Journal homepage: https://innovareacademics.in/journals/index.php/ijap

INTRODUCTION

Cancer's complexity spans biological interactions across various scales, urging its study within molecular, cellular, and physiological contexts. Computational cancer models address these challenges, aiding biological insights and clinical applications, utilizing chemotherapy drugs such as Doxorubicin, Paclitaxel, Cisplatin, Fluorouracil (5-FU), and Cyclophosphamide which are also used for colon cancer [1]. Colorectal Cancer (CRC) ranks as the third most frequently diagnosed cancer in both men and women in the United States. Over the past few decades, there has been a notable decline in both incidence and mortality rates. This decline can be attributed to various factors, including changes in risk behaviours such as reduced smoking and decreased consumption of red meat, widespread adoption of screening tests, and advancements in treatment modalities, particularly in reducing mortality rates [2]. Despite the high incidence of colorectal cancer, with an estimated 101,340 new cases of colon cancer and approximately 39,870 cases of rectal cancer expected, the combined mortality rate from these cancers is significant, with an estimated 49,380 deaths projected. However, there has been a notable decrease in the incidence per 100,000 of colon and rectal cancers, declining from 60.5 in 1976 to 46.4 in 2005. Additionally, mortality from colorectal cancer has decreased by almost 35% from 1990 to 2007, likely due to advancements in screening methods leading to earlier diagnosis and improved treatment options [3]. In 2023, the American Cancer Society projects that around 153,020 individuals will receive a diagnosis of CRC, with 52,550 deaths attributed to the disease. This includes 19,550 cases and 3,750 deaths occurring in individuals younger than 50 years old [4]. Thymidylate Kinase (TMPK) plays a crucial role in pyrimidine synthesis by catalyzing the phosphorylation of dTMP to form dTDP, which is further converted to Thymidine 5'-Triphosphate (dTTP). This enzyme is essential for DNA replication and is considered a potential drug target for various diseases, including Human immunovirus (HIV) and cancer. Inhibition of human TMPK has been shown to enhance the efficacy of anticancer agents like doxorubicin against colon cancer cells, irrespective of their p53 status [5]. TMPK utilizes Adenosine Triphosphate (ATP) as its phosphoryl donor in the reversible phosphorylation of Thymidine Monophosphate (TMP) to form Thymidine Diphosphate (TDP). Its position at the intersection of de novo and salvage pathways for Thymidine Triphosphate (TTP) synthesis underscores its significance in DNA replication, making it an attractive target for cancer chemotherapy. The enzyme's highly conserved P-loop motif aids in binding and positioning the phosphoryl donor and acceptor groups [6]. TMPK inhibitors, such as 3'-Azido-3'-Deoxythymidine 5'-O-Monophosphate (AZT-MP), have been investigated for their potential as antituberculosis agents. Studies have revealed competitive inhibition mechanisms of TMPK, with AZT-MP showing a Ki value of 10 µM [7]. Additionally, pyridino[d]isothiazolone inhibitors have been explored for their potential to target human thymidylate kinase as part of anti-cancer treatment strategies[8]. In the present work, we have targeted the charged residues Asp15, Arg70, and Glu152 at the base of the TMP-binding cavity and hydrophobic Phe105, and Phe72 of TMK [9]. We have designed tenligands from benzylidene derivatives. The designed ligands are 4-((2,4-hydroxybenzylidene)amino) phenol (C1), 4-((4-dichlorobenzylidene)amino)phenol (C2), 4-((4-nitrobenzylidene) amino)phenol (C3), 4-((4-methoxybenzylidene)amino)phenol (C4), 4-((4-fluorobenzylidene)amino)phenol (C5), 4-((4-chlorobenzylidene)amino)phenol (C6), 4-((4-bromobenzylidene) amino)phenol (C7), 4-((2-methylbenzylidene)amino)phenol (C8), 4-((2-methoxybenzylidene) amino) phenol (C9), 4-((4-(dimethyl amino) benzylidene) amino)phenol (C10).

MATERIALS AND METHODS

Molecular docking

Energy, score, and e-model values were pivotal in establishing the optimal docking pose for each ligand. Molecular docking, a computational technique, was employed to predict the binding behaviour and affinity of ligands towards the target enzyme [10]. Adjustments to the docked conformations were made based on the system's overall energy [11]. The selection of the X-ray crystallographic structure of human TMK (PDB ID: 1E2D, resolution: 1.65 Å) was foundational for this modelling work. The Schrödinger Suite 2021-4, through its Wizard module, facilitated the preparation of the protein [12]. This preparation process involved removing crystallographic water molecules by adding hydrogen [13]. The Prime tool within the Schrödinger Suite 2021-4 addressed any absent side chains, ensuring structural completeness. The OPLS3e force field was applied to optimize the system's energy, keeping the heavy atoms' root mean square deviation (RMSD) to a minimal 0.30 [14]. The delineation of the active site involved setting a radius of ten units around the centrally placed co-crystallized ligand within a grid box. The Glide tool, part of the suite, executed the docking of ten ligands, prepared with ligPrep, in XP mode, adhering to the default settings otherwise. These Glide parameters-energy, score, and e-model-were instrumental in identifying the most suitable docking pose for each ligand. Fig. 1 presents the protein-ligand complex, illustrating the results of this computational analysis.

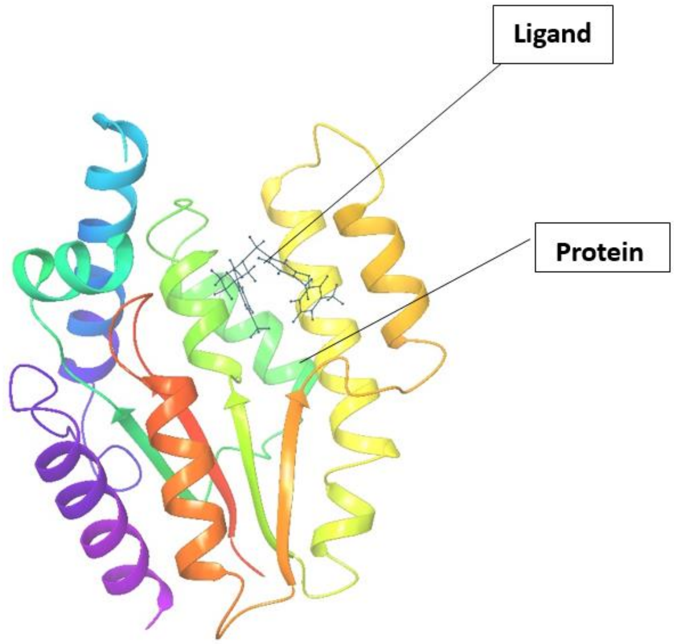

Fig. 1: Compound 1 protein-ligand interaction complex (PDB id: 1E2D) in molecular docking

Binding free energy calculations using prime MM-GBSA

Binding free energy for each protein-ligand duo was computed using the Prime MM-GBSA technique within the Schrödinger suite 2021-4. The energy minimization step utilized the OPLS3e force field along with the VSGB 2.0 solvation model [15]. This methodology includes advanced implicit solvation models that proficiently capture the nuances of hydrogen bonds, self-interactions, and hydrophobic forces, with an additional enhancement through a physics-based correction [16].

Study of molecular dynamic simulations

In our study, we employed time-step methodologies within the reference system propagator algorithm to address bonded and non-bonded electrostatic forces, whether they were short-range or long-range in nature. Data was systematically gathered at intervals of 100 picoseconds, and trajectory analyses were conducted to delve into the dynamics of the system [17]. Utilizing the Schrödinger suite 2021-4, MD simulations were carried out to scrutinize the nuclear binding dynamics of the top-rated compounds and to decode the molecular interactions at play [18]. For the simulation of the complex involving Compound 1 and the 1E2D structure, we adopted the TIP4P water model, setting up an orthorhombic box with periodic boundary conditions and a 10 Å buffer zone to separate protein atoms from the box edges [19]. The system's charge neutrality was achieved by adding 0.15 M NaCl counter ions. The energy minimization was refined using the OPLS4 force field. Long-range electrostatic interactions were precisely computed with the Ewald Smooth Particle Mesh Ewald technique, maintaining a tolerance threshold of 1e-09, while short-range van der Waals and Coulomb forces were assessed with a cut-off radius of 9.0 Å [20]. The study proceeded with 100 nanoseconds of MD simulations, maintaining a constant temperature of 300 Kelvin and pressure of 1 bar, employing the Isothermal-Isobaric (NPT) ensemble, which ensures a constant number of particles, temperature and pressure, albeit with variable volume. The simulation integrated the Nose-Hoover thermostat chain and the Martyna-Tobias-Klein barostat techniques at 100 and 200 picoseconds intervals for temperature and pressure stabilization, respectively [21, 22]. This multifaceted approach, leveraging multiple time-step methods, facilitated a thorough investigation into the behaviours and interactions of the complex compound 1/1E2D.

RESULTS

Binding free energy calculations and molecular docking

Leveraging the TMK structure (PDB ID: 1E2D), the Schrödinger Suite 2021-4 was utilized to authenticate docking studies through ligand-based virtual screening methodologies. The orientation of docked ligands matched precisely with the co-crystallized ligands, demonstrating an RMSD accuracy of 1.6 Å, as determined by the docking protocol. This process employed a virtual screening strategy to exclude functional groups that would potentially react adversely with the ligands by lipinski's Rule of Five. The XP-docking was evaluated based on several criteria including glide score, emodel, evdw, ecoul, and overall energy.

Table 1: The XP-docking score of compounds 1-10 in the catalytic pocket of (PDB id: 1E2D) thymidylate kinase(kcal/mol)

Comp. code	[a]gscore	[b]gemodel	[c]gevdw	[d]gecoul	[e]genergy
1	-6.33	-39.20	-26.17	-8.41	-34.59
2	-6.19	-43.38	-26.34	-3.11	-29.46
3	-6.18	-43.70	-30.28	-4.30	-34.58
4	-6.15	-55.17	-29.96	-8.15	-38.11
5	-6.14	-50.30	-31.31	-8.01	-39.32
6	-6.12	-50.58	-28.59	-9.49	-38.09
7	-6.06	-38.67	-29.19	-8.05	-37.24
8	-5.87	-57.63	-29.71	-4.94	-34.65
9	-5.85	-46.55	-29.58	-5.80	-35.39
10	-5.79	-47.55	-34.65	-2.34	-37.00

[a]glidescore, [b]glidemodelenergy, [c]glidevander waalsenergy, [d]glide coulombenergy, [e]glideenergy.

Table 1's docking data reveal that each ligand forms at least one hydrogen bond with amino acids, with glide scores spanning from -6.33 to-5.79 kcal/mol. In XP docking, compound 1 and compound 2 emerged with notable glide scores of -6.33 and -6.19 kcal/mol, respectively. Similarly, compound 3 and compound 4 demonstrated promising glide scores of -6.18 and -6.15 kcal/mol, respectively. Post-docking, the minimized binding free energies (ΔG_{Bind}) of these top-ranked poses showed an increase, ranging from -52.98 to -34.51 kcal/mol.

Table 2: Contribution of binding free energy (MM-GBSA) (kcal/mol) between compounds 1-10 (PDB id: 1E2D) thymidylate kinase complexes

Comp. code	[a]ΔGBind	[b]ΔGCoul	[c]ΔG_{HB}	[d]ΔGLip	[e]ΔGVdW
1	-52.98	12.54	2.25	-27.75	-47.70
2	-44.95	-5.92	1.06	-14.82	-39.43
3	-35.57	21.79	4.02	-24.24	-41.10
4	-40.28	5.89	2.81	-23.35	-38.87
5	-46.43	54.61	1.07	-19.09	-44.88
6	-49.70	-1.51	0.27	-19.66	-36.36
7	-44.82	8.04	-0.33	-19.20	-51.04
8	-48.99	32.35	1.94	-22.59	-57.92
9	-34.51	1.71	3.38	-20.39	-37.05
10	-43.85	-26.25	-1.34	-20.72	-44.26

[a]free energy of binding, [b]Coulomb energy, [c]hydrogen bonding energy, [d]hydrophobic energy (non-polar contribution estimated by solvent accessible surface area), [e]vander Waals energy.

Table 2 displays a significant range of Van der Waals energies (ΔG_{VdW}) from-36.36 to-57.92 kcal/mol and a range of hydrophobic energies (ΔG_{Lip}) from-14.82 to-27.75 kcal/mol, both contributing positively to the overall binding energy. Among the compounds, compound 1 achieved the highest glide score of -6.33 kcal/mol. Notably, compound 6 and compound 8 exhibited the most substantial binding affinities, with energies of -49.70 kcal/mol and -48.99 kcal/mol, respectively. In contrast, compound 1 demonstrated a binding affinity of -52.98 kcal/mol, as determined using the MM-GBSA method for critical free energy calculation. The 2D interactions of the compounds are illustrated in fig. 2.

Table 3: The number of hydrogen bonds and intermingling amino acid residues for the ten hits in the Thymidylate kinase catalytic pocket (PDB id: 1E2D)

Comp. code	Number of hydrogen bonds	Interacting amino acid residues
1	1	ASP15
2	2	GLU152, ARG76
3	1	GLU152
4	1	GLU152
5	1	GLU152
6	-	-
7	1	GLU152
8	1	GLU152
9	1	ASP15
10	1	ARG76

Table 3 details the hydrogen bonding interactions between designed molecules and specific amino acid residues. For Compound 1, notable interactions were observed with the amino acids Arg76, Tyr151, Phe105, Arg97, Phe72, and Asp15. Among these, Asp15 was identified as forming a hydrogen bond with Compound 1, making it a focus for further exploration based on both docking and binding affinity evaluations. In comparison to the rest, Compound 1, along with Compounds 2, 3, and 4, displayed superior outcomes. Notably, Compound 1 achieved a higher glide score than the other compounds, the co-crystal ligands, and the standard drug Doxycycline, as illustrated in fig. 3. This high glide score prompted a more detailed examination. Subsequently, we decided to conduct an in-depth MD simulation study on Compound 1, based on its promising glide score.

2D Interactions of molecules

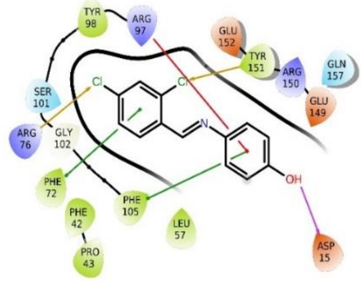

1

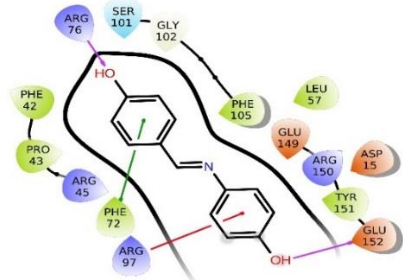

2

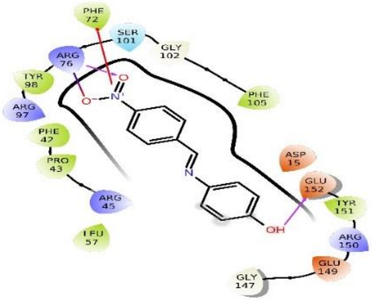

3

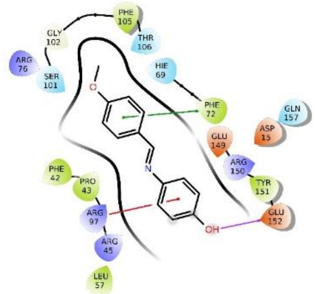

4

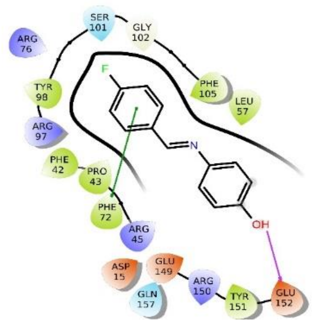

5

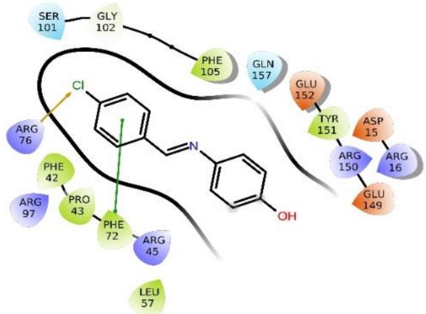

6

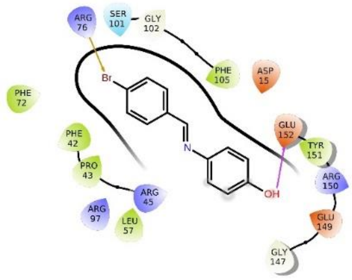

7

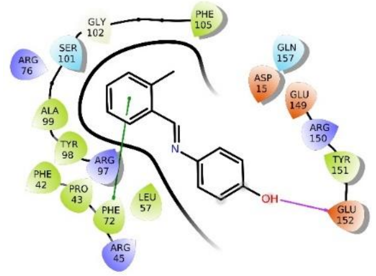

8

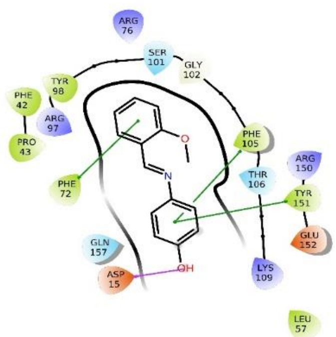

9

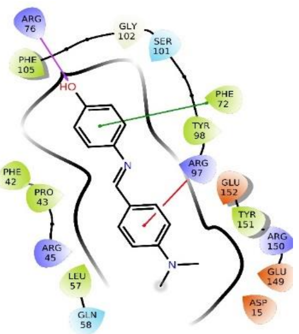

10

Fig. 2: **2D interaction diagrams of the ten chemicals in the thymidylate kinase catalytic pocket (PDB id: 1E2D)**

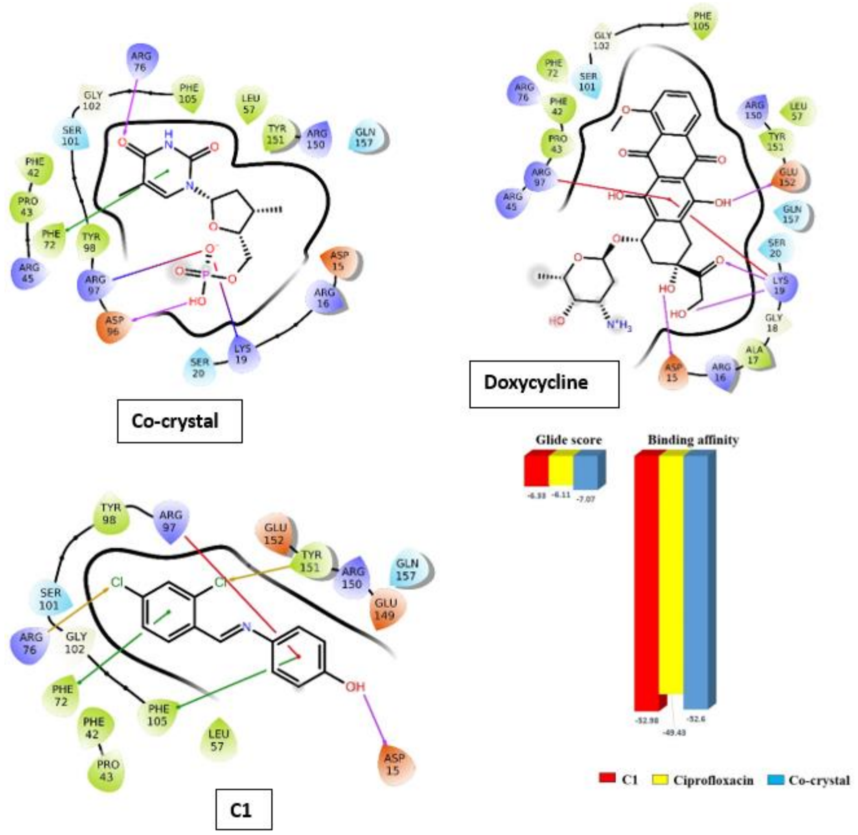

Fig. 3: Comparison of glide score and binding affinity between compound1, doxycycline, and Co-crystal

Illustrates the 2D interactions for all molecular hits. Compound 1 exhibits a glide score of-6.33 kcal/mol and a binding affinity of-52.98 kcal/mol.

MD simulation study

The molecular dynamic simulations of the ligand 4-((4-dichlorobenzylidene) amino)phenol, referred to as compound 1/1E2D, were conducted over a 100 ns period. This study provided insights into various metrics, including RMSD, root mean square fluctuations (RMSF), fractions of protein-ligand interactions, timelines of protein-ligand contacts, and a 2D diagram representing protein-ligand contacts. The stability of the docked pose for compound 1/1E2D was assessed through RMSD, focusing on the Cα atom's behavior and the fitting of the ligand (lig) to the protein (prot). The Cα atom displayed fluctuations between 0.5 to 1.6 Å, and the fit of the ligand to the protein exhibited a similar range of 0.6 to 1.6 Å. For 80 ns of the simulation, the Cα atom of the ligand achieved stability, while during the remaining 20 ns, it showed moderate stability. The fit of the ligand to the protein maintained stability for 90 ns. It exhibited moderate stability for the remaining 10 ns, contradicting the previously mentioned 20 ns, which seems to be a typo. The ligand demonstrated stable behavior from 0.6 to 1.6 Å between 20 ns to 80 ns. Meanwhile, moderate fluctuations for the ligand, ranging from 0.7 to 1.3 Å, were observed from 0 to 20 ns. These findings are illustrated in fig. 4.

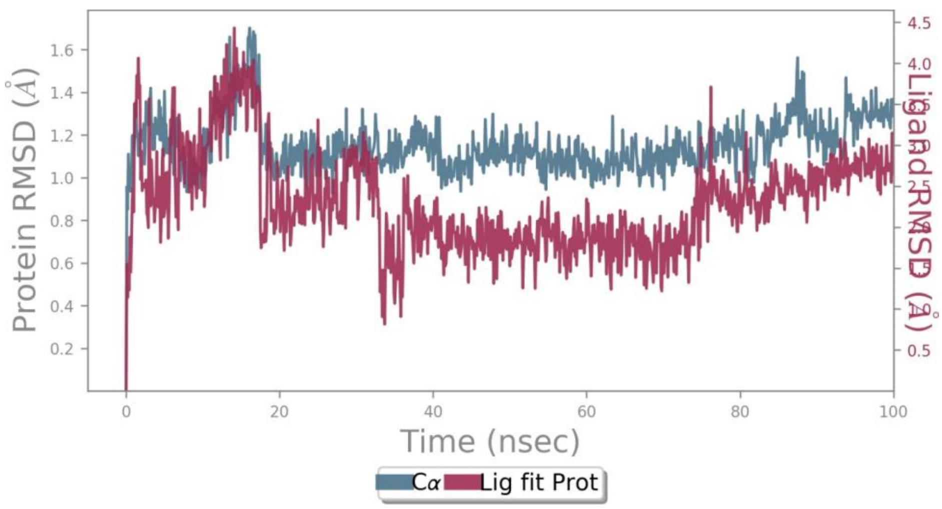

Fig. 4: RMSD graph for compound 1/E2D complex

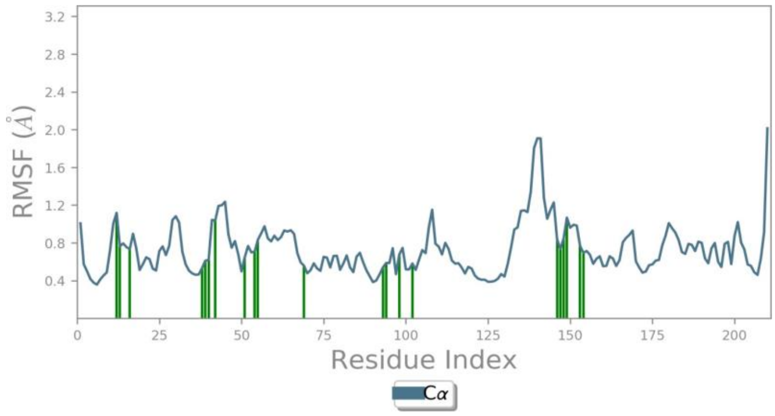

Fig. 5: RMSF diagram for compound 1/1E2D complex

In the RMSF analysis, minimal fluctuations were noted. The Cα atom exhibited initial fluctuations ranging from 0.4 to 1.0 Å, as shown in fig. 5, and this range was consistent throughout the simulations. Specific alterations in ligands interacting with amino acids were detected, with the highest stability recorded between 15 to 155 ns. The period from 150 to 155 ns showed the lowest fluctuations, with amino acid RMSF values between 0.7 to 1.1 Å.

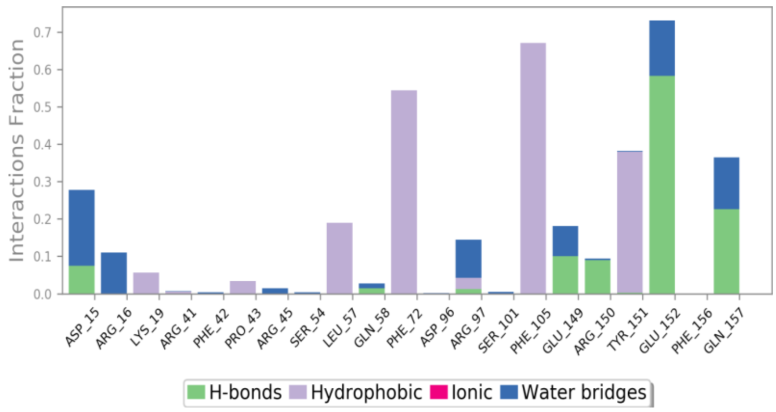

Fig. 6: Protein-ligand contacts profile for compound 1/1E2D complex

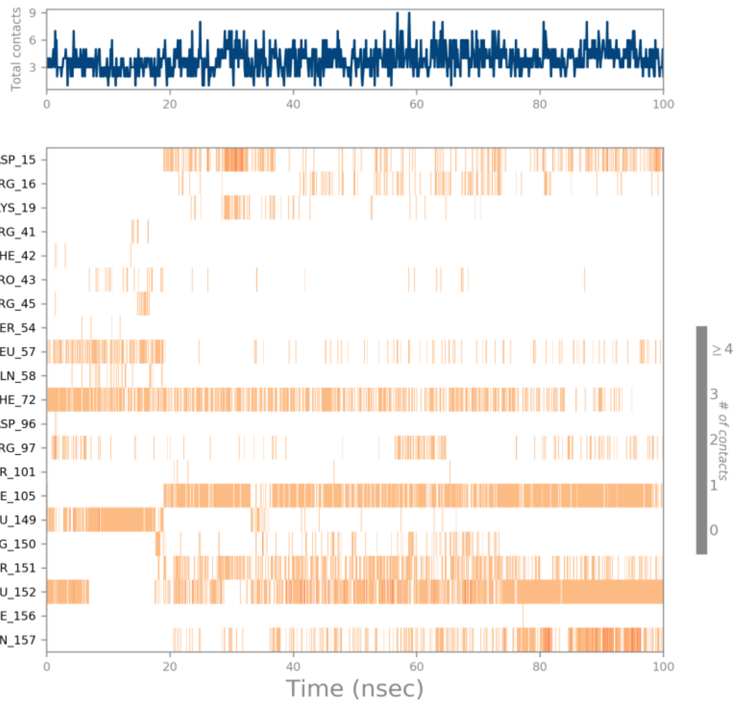

Fig. 7: **Timeline representation for compound 1/1E2D complex**

Fig. 7 demonstrates that Phe72 was in consistent contact with the ligands for 90 out of 100 nanoseconds. Similarly, Phe105 was in continuous contact with the ligands from 20 to 100 ns. Tyr151 and Glu152 also maintained uninterrupted contact with the ligands throughout the same period, from 20 to 100 ns. The protein-ligand interactions are depicted in the 2D diagram presented in fig. 8.

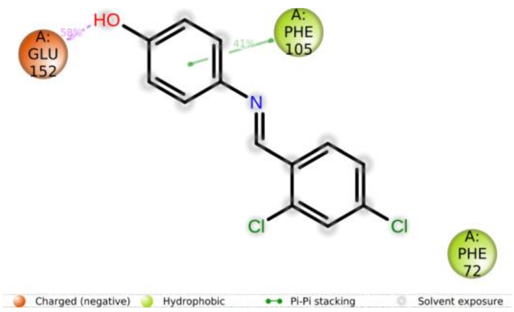

Fig. 8: **2D diagram for compound 1/1E2D complex**

Phe105 consistently interacted with the aromatic ring through pi-pi stacking, maintaining a stable bond 41% of the time. Meanwhile, Glu152 was in constant contact with the hydroxy group via a hydrogen bond, with this interaction remaining stable at 58%, as illustrated in fig. 8. Based on these findings, the ligand compound 1 exhibits promising potential for the development of new anticancer agents.

DISCUSSION

Previous studies have extensively investigated the inhibition of TMK, an enzyme involved in nucleotide biosynthesis, as a potential therapeutic strategy for various diseases, including cancer and infectious diseases caused by bacteria and viruses. Several classes of compounds have been identified as potential inhibitors of TMK, demonstrating promising inhibitory activity in silico studies. Among the inhibitors studied, pyridine-fused and arene-fused isothiazolone analogues have shown strong potential as inhibitors targeting the HaTMK. The pyridine-fused analogue exhibited a high binding affinity for the B-site of HaTMK, interacting with key residues such as Ala145 and Glu149 through hydrogen bonding. Additionally, it engaged with the lID region of the enzyme and demonstrated stability during molecular dynamics simulations. On the other hand, the arene-fused analogue showed an affinity for both the B-site and D-site of HaTMK, indicating its potential as a dual-site inhibitor [23]. In other studies, inhibitors targeting TMK in different organisms have been explored. For instance, dihydropyrimidinones have been investigated as inhibitors targeting TMK in *Mycobacterium Tuberculosis* (TB), with a focus on residues such as Arg167, Arg74, and Phe70 [24]. Triazole and pyrimidine derivatives have been studied as inhibitors targeting TMK in *Staphylococcus aureus*, with a particular emphasis on residues Arg70, Ser97, Gln101, and Arg48 [25]. Similarly, 3-methoxythyamine-β-xanthin derivatives have been examined as inhibitors targeting TMK in the *monkeypox virus*, with a focus on residues lys14, Phe38, Arg93, and Glu145 [26]. In addition, luteolin and rosmarinic acid have been explored as inhibitors targeting TMK in both bacterial and cancer cells. These compounds have shown promising inhibitory activity, with interactions observed with residues such as Gly22, Arg303, Asp42, leu214, His215, and Gly249 [27]. Furthermore, imidazole rings with NH_2 group derivatives have been studied as inhibitors targeting TMK in the *Variola virus*, targeting residues Asn65, Arg93, Glu116, Asp13, and Arg93 [28]. lastly, β-thymidine derivatives have been investigated as inhibitors targeting TMK in *Plasmodium falciparum*, demonstrating a remarkable binding affinity and specificity for the enzyme. These inhibitors targeted residues such as Arg78, Arg99, Arg47, Tyr153, Ser106, and Asp17 [29]. This study introduces novel benzylidene aminophenol compounds synthesized by our team. We explored various substituted benzylidene aminophenols, which exhibited promising binding affinity with the TMK protein in *in silico* studies. While TMK enzyme has been a target for cancer treatment, there is a lack of research on colon cancer using benzylidene aminophenol derivatives as drugs. Thus, our investigation into benzylidene aminophenol derivatives for targeting TMK enzyme in colon cancer represents a novel approach.

Our study specifically focuses on colon cancer, recognizing that TMK enzymes are present in colon cancer cells. After obtaining favorable binding affinity results in *in silico* studies targeting TMK enzyme, our next step involves formulating these compounds to target colon cancer cells. We anticipate that these compounds may serve as active drugs for colon cancer treatment. Past studies have shown that compounds exhibiting good binding affinity in *in silico* studies were further developed and targeted for different cancers, underscoring the potential of benzylidene aminophenol derivatives as promising candidates for colon cancer treatment [8]. The detailed understanding of the interactions between these inhibitors and TMK provides valuable insights for the development of novel therapeutic agents targeting various diseases.

CONCLUSION

The investigation into benzylidene amino phenol derivatives has highlighted their potential as strong contenders for developing anti-colon cancer medications. Among these, Compound 1, namely 4-((4-dichlorobenzylidene) amino)phenol, stood out for its remarkable properties, achieving a notable glide score of-6.33 kcal/mol and a binding affinity of-52.98 kcal/mol. MD simulations indicated that this compound maintained its stability throughout 80 ns of a 100 ns simulation, showcasing a backbone atom RMSD stability at 1.6 Å. The interaction of Compound 1 with Glu152 through a hydroxy group, alongside continuous contact with amino acids such as Phe105, Phe72, Tyr151, and Glu152, underscores its potential mechanism for inhibiting enzyme activity, pointing towards a viable anti-cancer strategy. Comparatively, this compound exhibits higher binding affinities than other studied analogues, such as pyridine-fused and arene-fused isothiazolone analogues, which target the same enzyme but with less efficacy. Additionally, compared to β-thymidine derivatives, Imidazole rings with NH2 group derivatives, luteolin and Rosmarinic acid, 3-Methoxytyramine-β-xanthin derivatives, and Triazole and pyrimidine derivatives reported for different bacterial TMK, our benzylidene amino phenol derivatives show superior promise. This suggests that our derivatives could also be effective against colon cancer, based on these comparative insights. Moving forward, the focus will be on further exploring these derivatives for colon cancer treatment through formulation studies, positioning benzylidene amino phenol derivatives at the forefront of anti-colon cancer drug development. Nevertheless, additional experimental research is required to fully validate their therapeutic potential and safety.

ACKNOWLEDGMENT

The authors would like to thank the Department of Pharmaceutical Biotechnology and Department of Pharmaceutical Chemistry, JSS College of Pharmacy, Ooty, Tamil Nadu, for providing facilities for conducting Research.

FUNDING

No funding was received for this work.

AUTHORS CONTRIBUTIONS

Mohd Abdul Baqi-Conceptualization, validation, writing-original draft preparation and Data curation.

Koppula Jayanthi-Data curation, methodology, writing-Review and Editing.

Raman Rajeshkumar-Conceptualization, Formal analysis, validation, and supervision.

CONFLICT OF INTERESTS

Declared none

REFERENCES

1. Edelman LB, Eddy JA, Price ND. In silico models of cancer. Wiley Interdiscip Rev Syst Biol Med. 2010 Jul;2(4):438-59. doi: 10.1002/wsbm.75, PMID 20836040.

2. Siegel RL, Miller KD, Fedewa SA, Ahnen DJ, Meester RG, Barzi A. Colorectal cancer statistics, 2017. CA Cancer J Clin. 2017 May 6;67(3):177-93. doi: 10.3322/caac.21395, PMID 28248415.
3. Labianca R, Beretta G, Gatta G, de Braud F, Wils J. Colon cancer. Crit Rev Oncol Hematol. 2004;51(2):145-70. doi: 10.1016/j.critrevonc.2004.03.003, PMID 15276177.
4. Siegel RL, Wagle NS, Cercek A, Smith RA, Jemal A. Colorectal cancer statistics, 2023. CA Cancer J Clin. 2023 May;73(3):233-54. doi: 10.3322/caac.21772, PMID 36856579.
5. Cui Q, Shin WS, Luo Y, Tian J, Cui H, Yin D. Thymidylate kinase: an old topic brings new perspectives. Curr Med Chem. 2013;20(10):1286-305. doi: 10.2174/0929867311320100006, PMID 23394555.
6. Ostermann N, Schlichting I, Brundiers R, Konrad M, Reinstein J, Veit T. Insights into the phosphoryltransfer mechanism of human thymidylate kinase gained from crystal structures of enzyme complexes along the reaction coordinate. Structure. 2000;8(6):629-42. doi: 10.1016/s0969-2126(00)00149-0, PMID 10873853.
7. Sukumar S, Krishman A, Khan MK. Protein kinases as antituberculosis targets: the case of thymidylate kinases. Front Biosci (Landmark Ed). 2020;25(9):1636-54. doi: 10.2741/4871, PMID 32114448.
8. Chen YH, Hsu HY, Yeh MT, Chen CC, Huang CY, Chung YH. Chemical inhibition of human thymidylate kinase and structural insights into the phosphate binding loop and ligand-induced degradation. J Med Chem. 2016 Nov 10;59(21):9906-18. doi: 10.1021/acs.jmedchem.6b01280, PMID: 27748121.
9. Ostermann N, Schlichting I, Brundiers R, Konrad M, Reinstein J, Veit T. Insights into the phosphoryltransfer mechanism of human thymidylate kinase gained from crystal structures of enzyme complexes along the reaction coordinate. Structure. 2000;8(6):629-42. doi: 10.1016/s0969-2126(00)00149-0, PMID 10873853.
10. James JP, Aiswarya TC, Priya S, Jyothi D, Dixit SR. Structure based multitargeted molecular docking analysis of pyrazole-condensed heterocyclics against lung cancer. Int J App Pharm. 2021;3(6):157-69. doi: 10.22159/ijap.2021v13i6.42801.
11. Dar AM, Mir S. Molecular docking: approaches, types, applications and basic challenges. J Anal Bioanal Tech. 2017;08(2):1-3. doi: 10.4172/2155-9872.1000356.
12. Sastry GM, Adzhigirey M, Day T, Annabhimoju R, Sherman W. Protein and ligand preparation: parameters, protocols, and influence on virtual screening enrichments. J Comput Aided Mol Des. 2013 Mar;27(3):221-34. doi: 10.1007/s10822-013-9644-8, PMID 23579614.
13. Sunitha Sukumaran, Meghna M, Sneha S, Arjun B, Sathianarayanan S, Saranya T S. Insilico analysis of acridone against TNF-α and PDE4 targets for the treatment of psoriasis. IJRPS. 2020;11(SPL4):1251-9. doi: 10.26452/ijrps.v11iSPL4.4286.
14. Dunkel M, Fullbeck M, Neumann S, Preissner R. Super natural: a searchable database of available natural compounds. Nucleic Acids Res. 2006;34:D678-83. doi: 10.1093/nar/gkj132, PMID 16381957.
15. Jacobson MP, Pincus DL, Rapp CS, Day TJ, Honig B, Shaw DE. A hierarchical approach to all-atom protein loop prediction. Proteins. 2004 May;55(2):351-67. doi: 10.1002/prot.10613, PMID 15048827.
16. Dhawale S, Gawale S, Jadhav A, Gethe K, Raut P, Hiwarale N. In silico approach targeting polyphenol as fabh inhibitor in bacterial infection. Int J Pharm Pharm Sci. 2022;14(11):25-30. doi: 10.22159/ijpps.2022v14i11.45816.
17. Martyna GJ, Tuckerman ME, Tobias DJ, Klein ML. Explicit reversible integrators for extended systems dynamics. Mol Phys. 1996;87(5):1117-57. doi: 10.1080/00268979600100761.
18. Guo Z, Mohanty U, Noehre J, Sawyer TK, Sherman W, Krilov G. Probing the alpha-helical structural stability of stapled p53 peptides: molecular dynamics simulations and analysis. Chem Biol Drug Des. 2010;75(4):348-59. doi: 10.1111/j.1747-0285.2010.00951.x, PMID 20331649.
19. Essmann U, Perera L, Berkowitz ML, Darden T, Lee H, Pedersen LG. A smooth particle mesh ewald method. Journal of Chemical Physics. 1995;103(19):8577-93. doi: 10.1063/1.470117.
20. Harder E, Damm W, Maple J, Wu C, Reboul M, Xiang JY. OPLS3: a force field providing broad coverage of drug-like small molecules and proteins. J Chem Theory Comput. 2016;12(1):281-96. doi: 10.1021/acs.jctc.5b00864, PMID 26584231.
21. Martyna GJ, Tobias DJ, Klein ML. Constant pressure molecular dynamics algorithms. Journal of Chemical Physics. 1994;101(5):4177-89. doi: 10.1063/1.467468.
22. Badavath VN, Sinha BN, Jayaprakash V. Design, *in silico* docking and predictive ADMEproperties of novel pyrazoline derivatives with selective human MAO inhibitory activity. Int J Pharm Pharm Sci. 2015;7:277-82.
23. Chen YH, Hsu HY, Yeh MT, Chen CC, Huang CY, Chung YH. Chemical inhibition of human thymidylate kinase and structural insights into the phosphate binding loop and ligand-induced degradation. J Med Chem. 2016;59(21):9906-18. doi: 10.1021/acs.jmedchem.6b01280, PMID 27748121.
24. Vedula GS, Nemala SK. In silico molecular docking studies of di hydro pyrimidinones as MTB thymidylate kinase inhibitors. IJHS. 2022;6(S4)4966-76, doi: 10.53730/ijhs.v6nS4.9216.
25. Qureshi B, Khalil R, Saeed M, Nur-e-Alam M, Ahmed S, Ul-Haq Z. Structure-based discovery of potent staphylococcus aureus thymidylate kinase inhibitors by virtual screening. Med Chem. 2022;19(1):75-90. doi: 10.2174/1573406418666220407092638, PMID 35392789.
26. Khan A, Adil S, Qudsia HA, Waheed Y, Alshabrmi FM, Wei DQ. Structure-based design of promising natural products to inhibit thymidylate kinase from monkeypox virus and validation using free energy calculations. Comput Biol Med. 2023;158:106797. doi: 10.1016/j.compbiomed.2023.106797, PMID 36966556.
27. Faisal S, Tariq MH, Ullah R, Zafar S, Rizwan M, Bibi N. Exploring the antibacterial, antidiabetic, and anticancer potential of Mentha arvensis extract through in silico and *in vitro* analysis. BMC Complement Med Ther. 2023 Jul 26;23(1):267. doi: 10.1186/s12906-023-04072-y, PMID 37496047.
28. Rodrigues Garcia D, Rodrigues De Souza F, Paula Guimaraes A, Castro Ramalho T, Palermo De Aguiar A, Celmar Costa França T. Design of inhibitors of thymidylate kinase from *Variola virus* as new selective drugs against smallpox: part II. J Biomol Struct Dyn. 2019 Nov 22;37(17):4569-79. doi: 10.1080/07391102.2018.1554510, PMID 30488769.
29. Kandeel M, Kitade Y, Al-Taher A, Al-Nazawi M. The structural basis of unique substrate recognition by plasmodium thymidylate kinase: molecular dynamics simulation and inhibitory studies. PLOS ONE. 2019;14(2):e0212065. doi: 10.1371/journal.pone.0212065, PMID 30730992.